NOTICE CONCERNING COPYRIGHT RESTRICTIONS

Comparison of Traveltime Delay with Well Pressure Decline Sonic Logs in the Higashi-Hachimantai Geothermal Field

Hiroyuki Saito, S. Suzuki and Kazuo Hayashi

Institute of Fluid Science, Tohoku University
SENDAI 980-8577, Japan

ABSTRACT

A data set of pressure decline sonic logs was used to monitor the reopening behavior of a hydraulic single fracture in the Higashi-Hachimantai geothermal field. In the measurement, a single receiver was deployed as a sonic tool with a 3ft source-receiver interval. The source center frequency is 15kHz. The waveform was recorded at intervals of 0.1m to assure high depth resolution, maintaining well EE-4's wellhead pressure at 3MPa, 1MPa and 0MPa. To estimate traveltime delays of P-wave and S-wave accurately, the cross-spectrum method was applied. Data analysis indicates that there is a strong correlation between the wellhead pressure and P-wave and S-wave traveltime delays at the depth of the fracture; that is, the P-wave and S-wave traveltime delays increase as wellhead pressure increase. Another important phenomenon was that the P-wave and S-wave traveltime delays also observed in the fracture vicinity. If this were correct, a large process zone would be expected in the fracture vicinity. The pressure decline sonic logs indicate complicated processes occurring during hydraulic fracturing that have significant implications for geothermal energy extraction.

Introduction

Reservoir performance of the engineered geothermal systems such as HDR (Duchane, 1991) and HWR (Takahashi and Hashida, 1992) is dominated by the fracture system, both natural and hydraulically induced; therefore it is essential to estimate the characteristics of fracture system.

The Geothermal Energy Extraction Engineering Group (GEEE) of Tohoku University has continued studies on development of new fracture characterization methods and a comprehensive set of experiments was carried out to investigate the characteristics of an artificial subsurface fracture induced hydraulically in Higashi-Hachimantai Hot Dry Rock field (Niitsuma, 1989). Right after the hydraulic fracturing, the artificial fracture was considered as a single narrow fracture oriented orthogonal to the direction of least principal stress as determined from continuous drilled cores and the result of impression packer measurement at the fracture depth in well EE-4. Niitsuma and Saito (1991a) observed P-wave travel time increase during pressurization of the fracture by the interwell seismic measurements, and they explained this phenomenon by a model considering the reopening of micro-cracks in the vicinity of the main fracture. Since then, field studies by means of interwell seismic measurement have provided evidence that the artificial fracture is embedded in a hydraulically communicating zone (Moriya and Niitsuma, 1995; Tanaka *et al.*, 1999).

To investigate the detailed properties of the fracture system, full waveform acoustic logging (FWAL) was carried out while pressurizing the fracture. Saito and Hayashi (1999) clarified the process zone's thickness in the fracture vicinity as a function of the wellhead pressure from the observed attenuation interval of P-wave and borehole Stoneley. But more detailed studies are necessary to understand the properties of a fracture system in geothermal field.

In this paper, we present some of the results for the change of P-wave and S-wave traveltime delay observed in the well pressure decline FWAL data, have provided important clues to the fracture system and the fracturing process in the Higashi-Hachimantai field.

Experiment

Higashi-Hachimantai Hot Dry Rock field for this study is located in Iwate Prefecture, Japan. Figure 1 (overleaf) shows the location and the schematic of the Higashi-Hachimantai field. A subsurface fracture was created at a depth of 369.0m in well F-1 by hydraulic fracturing. The bedrock in which the artificial fracture was created is an intact welded tuff, which has no significant joints or fractures within the depth interval of 280-380m. Well EE-4 was drilled into the fracture after the fracturing, and intersected at a depth of 358.2m. The strike and dip of the fracture in well EE-4 are N61°E and 46°NW, respectively. From the injection volume of propping agent, the fracture diameter was estimated to be 50m. The relation between the fracture aperture and the wellhead pressure in this artificial fracture was estimated by a transmissivity test (Hayashi and Abé, 1989), and

the fracture aperture was about 0.1mm without pressurization and 0.2mm at a wellhead pressure of 3.0MPa. The 3-D configuration of the fracture was estimated by the triaxial shear-shadow method (Niitsuma and Saito, 1991b).

Well pressure decline FWAL measurements were carried out in the depth range of 330-360m in well EE-4. A conventional single receiver was deployed as an acoustic logging tool with a 3ft source-receiver interval. The source center frequency is 15kHz. The fracture aperture was controlled by injection of water into the well F-1 by a pump on the surface. The wellhead of well EE-4 was shut with a wireline lubricator. Three FWAL logs were obtained maintaining well EE-4's wellhead pressure at 0MPa, 1MPa and 3MPa. The waveform was recorded at intervals of 0.1m to assure high depth resolution.

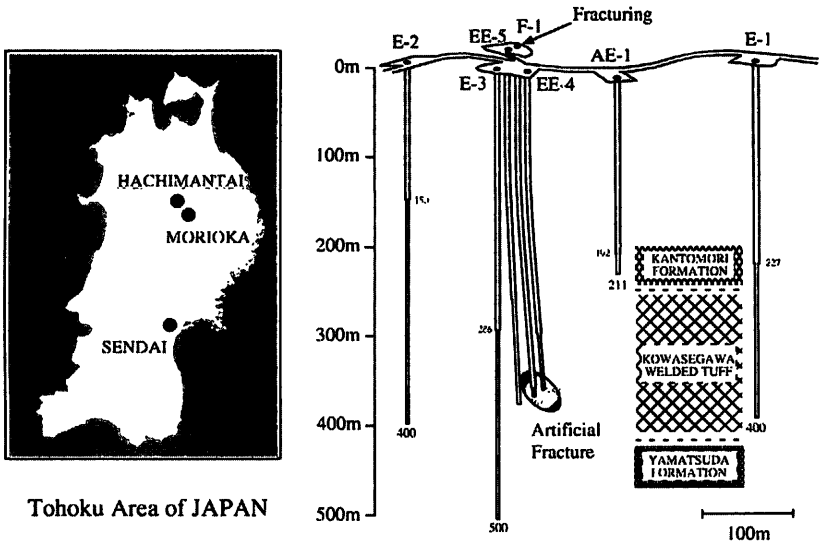

Figure 1. Location map and schematic of the Higashi-Hachimantai Hot Dry Rock field. Well EE-4 and well F-1 intersects an artificial subsurface fracture at depths of 358.2m and 369.0m, respectively.

Traveltime Delay Estimation

In acoustic data processing, the arrival pick is made at an arbitrary point within the first quarter cycle of the first arrival for the effect of gain adjustment on the arrival pick. For this reason, the arrival pick is postponed to take the first zero crossing after the amplitude threshold has been achieved, rather than picking at the amplitude threshold (Paillet and Cheng, 1991). Such a scheme produces a consistent phase at arrival-time but difference in waveform shape can cause errors. The errors become much more severe when fracture attenuates the waveform. In the case of our study, the aim of signal analysis is to extract the traveltime delay, rather than the exact arrival-time. Hence, we used cross spectrum analysis to detect the traveltime delay of P-wave and S-wave in frequency domain.

The basic method of cross-spectrum analysis was originally described by Poupinet *et al.* (1984), and applied to AE/MS analysis (Moriya *et al*, 1994) and interwell seismic data analysis (Tanaka *et al*, 1999). Therefore, we briefly outline the method. The cross spectrum $S_{ab}(f)$ of the two acoustic signals $a(t)$ and $b(t)$ for a given time window is defined by equation (1).

$$S_{ab}(f) = K_{ab}(f) - jQ_{ab}(f) \tag{1}$$

where, $K_{ab}(f)$ and $Q_{ab}(f)$ are the cospectrum and the quadrature spectrum two windowed signals at elapsed time t, j is $\sqrt{-1}$.

The phase $\psi_{ab}(f)$ of $S_{ab}(f)$ is defined as:

$$\psi_{ab}(f) = \tan^{-1}\left(Q_{ab}(f)/K_{ab}(f)\right) \tag{2}$$

and the relative time delay $\tau_{ab}(t)$ as

$$\tau_{ab}(t) = \psi_{ab}/2\pi f \tag{3}$$

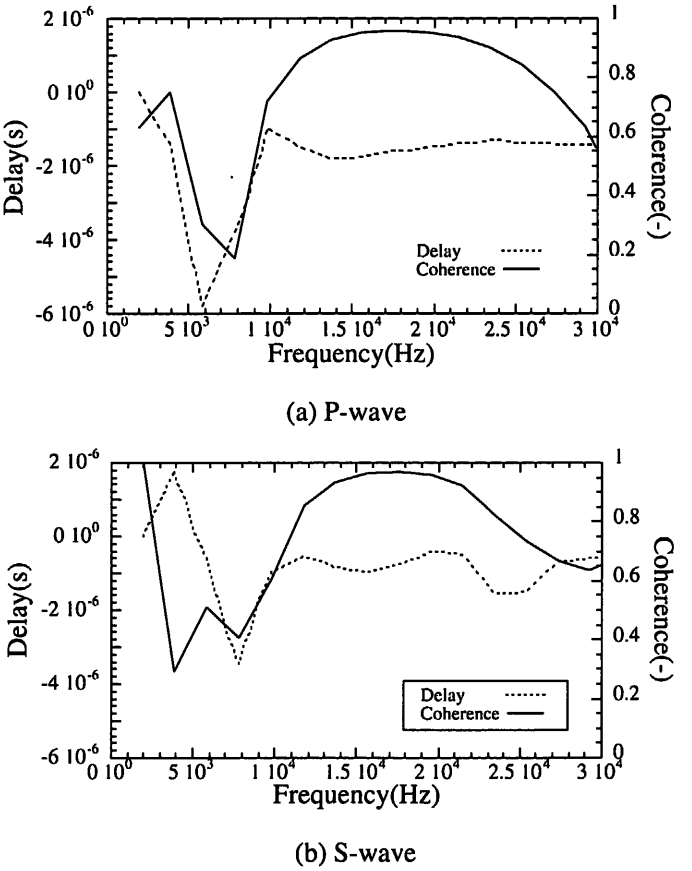

Figure 2. Examples of the estimated traveltime delay and coherence. (a) P-wave's example of traveltime delay and coherence. (b) S-wave's example of traveltime delay and coherence.

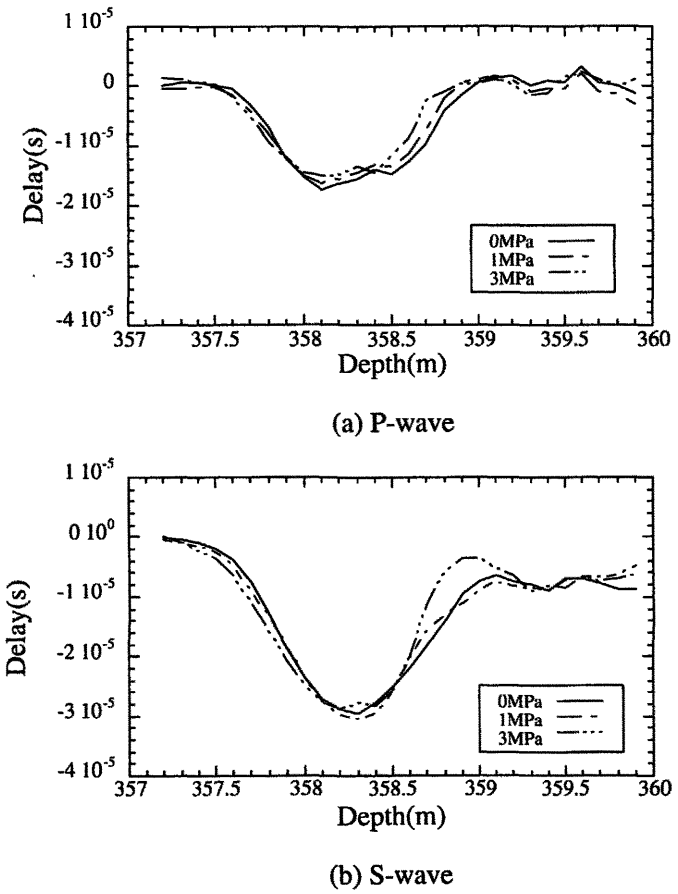

Figure 3. Traveltime delays at the well EE-4's wellhead pressure of 0MPa, 1MPa and 3MPa. Depth range is 357-360m. (a) Traveltime delay of P-wave. (b) Traveltime delay of S-wave.

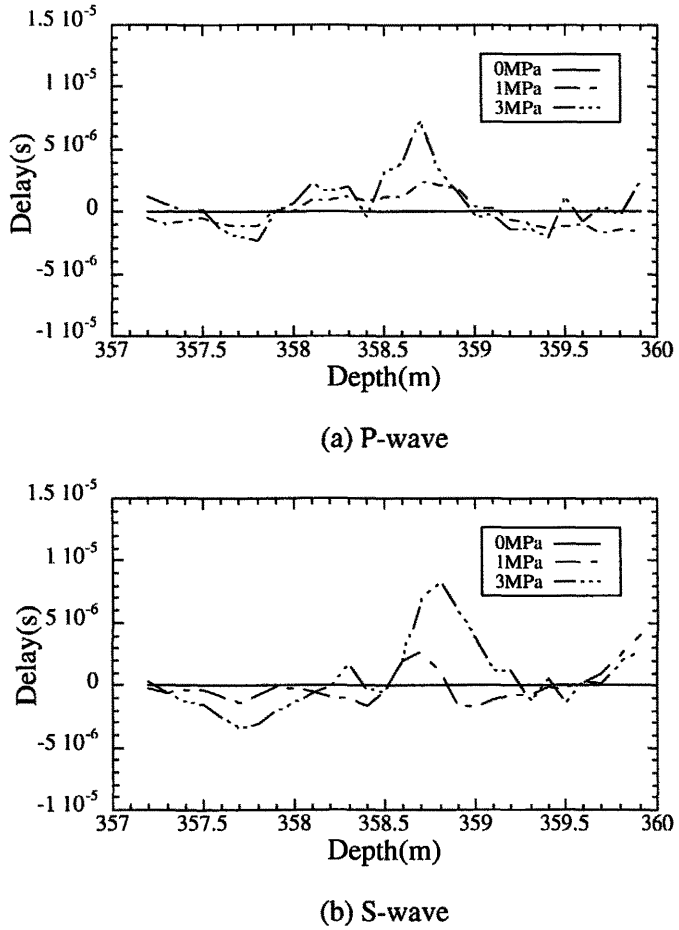

Figure 4. Difference of the traveltime delays in the well EE-4's wellhead pressure of 0MPa, 1MPa and 3MPa. (a) Difference of the P-wave's traveltime delay. (b) Difference of the S-wave's traveltime delay.

and the coherence magnitude spectrum coh(f) using the cross spectrum and the autospectra as

$$coh(f)^2 = \frac{|S_{ab}(f)|^2}{S_{aa}(f)S_{bb}(f)} \quad (4)$$

where, $S_{aa}(f)$ and $S_{bb}(f)$ are the autospectra of the two signals. $coh(f)$ ranges from 0 to 1 and is an estimator of the similarity of the signals around a given frequency.

We used the Blackman-Tukey method for Fourier Transform, where the time window length are 0.2ms for P-wave and 0.18ms for S-wave. Figure 2(a) shows an example of the estimated relative time delays and the coherence for P-wave, and Figure 2(b) shows that for S-wave. We averaged the relative time delays in the frequency range 13-17kHz based on the dominant frequency range of the signals of 13-17kHz, and the coherence indicates stable value higher than 0.9 in the frequency range.

Result and Discussion

Figure 3(a) and Figure 3(b) show the traveltime delay of P-wave and S-wave at the Well EE-4's wellhead pressure of 0MPa, 1MPa and 3MPa, respectively. The depth range is 357.0-360.0m. We used a signal of 357.0m depth at the Well EE-4's wellhead pressure of 0MPa as a reference signal, so that the estimated delays were the relative delays to the reference signal. The travel time delays of P-wave and S-wave fall down to lowest value at around 358.0m. The change of traveltime may be caused by formation velocity change or effect of a fracture on in situ stresses. But there is no clear formation change in Well EE-4's drilled cores of the corresponding depth. The relationship between traveltime of seismic waves and effect of a fracture on in situ stress is under consideration.

Another feature of Figure 3(a) and Figure 3(b) is that the traveltime delays of P-wave and S-wave in the depth range of 358.5-359.0m increase as the Well EE-4's wellhead pressure increase. Figure 4(a) is the difference of P-wave traveltime delay in the Well EE-4's wellhead pressure between 0MPa and 1MPa, 0MPa and 3MPa. Figure 4(b) is the difference of S-wave traveltime delay. There is a slight increase of the difference of the P-wave traveltime delay in the depth range of 357.7-359.4m, and an increase of the S-wave difference is only around 358.7m. Both of the traveltime delay's differences rise to peak at the depth of about 358.7m, which is in agreement with the maximum of the P-wave amplitude deficit observed by Saito and

Hayashi (1999). The maximums of the P-wave traveltime delay's difference to 0MPa are 2.4μs at 1MPa and 7.4μs at 3MPa. And those of S-wave are 2.6μs at 1MPa and 8.4μs at 3MPa.

Next, we estimated the change of fracture aperture by integrating a simple solid/fluid/solid interface model and the detected traveltime delay's difference. Figure 5 shows the traveltime delay as a function of the fracture aperture with the physical properties of the Higashi-Hachimantai field. Table 1 shows the physical properties of the Higashi-Hachimantai field. We obtained the fracture aperture with the least square method, fitting the detected traveltime delay's difference to the theoretical curves in Figure 5. Figure 6 shows the estimated fracture aperture and the estimated fracture aperture from the amplitude deficit of borehole Stoneley wave (Saito and Hayashi, 1999). As shown in Figure 6, there is a significant difference in the estimated fracture apertures of 3MPa between the traveltime delay and the Borehole Stoneley wave; the estimated fracture apertures are nearly equal at 0MPa and 1MPa, however. Considering that the reopening pressure of the fracture is about 2MPa (Hayashi and Abé, 1989) and the amplitude deficit of borehole Stoneley wave is an indicator of fracture permeability (Tang and Cheng, 1989), this fact suggests that the traveltime delay observed at 1MPa is caused mainly by the permeation of injected water into the process zone. In the case of 3MPa, the pore dilatancy in the process zone is dominant because the estimated fracture from the traveltime delay is larger than that from the borehole Stoneley wave.

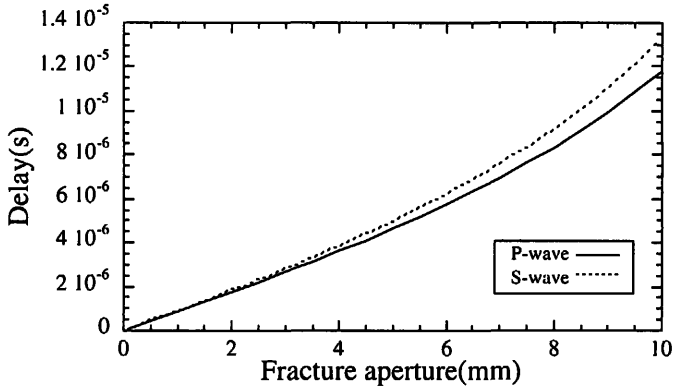

Figure 5. Theoretical traveltime delays by a simple solid/fluid/solid interface model.

Table 1. Physical parameters used in this study.

P-wave velocity (formation)	2710 (m/sec)
S-wave velocity (formation)	1730 (m/sec)
Density (formation)	2300 (kg/m^3)
Acoustic velocity (water)	1500 (m/sec)
Density (water)	1000 (kg/m^3)

Conclusion

We have estimated the traveltime delays of P-wave and S-wave with the well pressure decline sonic logs in the Higashi-Hachimantai field, using the cross spectrum method.

The P-wave traveltime delays were observed at the depth range of 357.7-359.4m at the pressure of pressures of under reopening pressure, and the traveltime delays of P-wave and S-wave increase as wellhead pressure increase. This is one of the strongest evidence of a wide process zone surrounding the main fracture and the micro fractures in the process zone are hydraulically well connected.

The fracture aperture obtained from the traveltime delays are nearly equal to that obtained from borehole Stoneley wave when the pressure is under the reopening pressure of the fracture. But the fracture aperture obtained from the traveltime delays

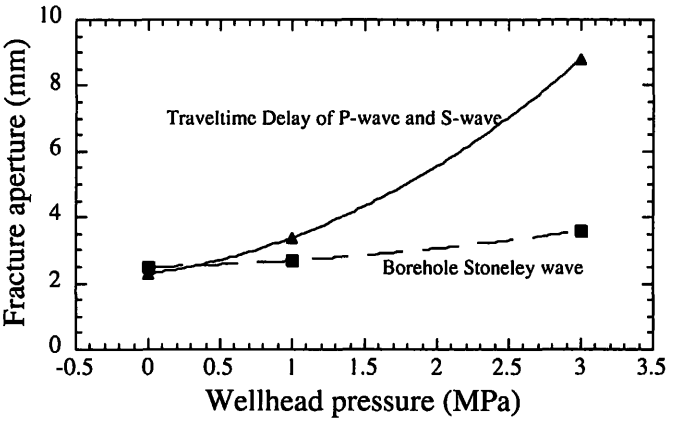

Figure 6. Comparison of estimated fracture aperture between the result of traveltime delay and that of amplitude deficit of borehole Stoneley wave.

is larger than that obtained from borehole Stoneley wave when the pressure is over the reopening pressure. Such a phenomenon make it possible to interpret that the traveltime delay at the pressure of under the reopening pressure is caused by the permeation of injected water into the process zone, and that of over the reopening pressure is caused by the pore dilatancy in the process zone.

Acknowledgement

The present work was supported by JSPS (Japan Society for Promotion Science) through a Grant-in-Aid for Scientific Research (No.12750826) and partially supported by NEDO (New Energy and Industrial Development of Japan) under International Joint Research Grant "MURPHY Project".

References

Blackman, R. B. and Tukey, J. W. (1958). The measurement of Power Spectra from the Point of View of Communication Engineering, *Dover Publication Inc.*

Duchane, D. (1991). International Programs in Hot Dry Rock Technology Development. *Geother. Resour. Coun. Bull.*, 20, pp.135-142.

Hayashi, K. and Abé, H., (1989). Evaluation of Hydraulic Properties of the Artificial Subsurface System in Higashihachimantai Geothermal Model Field, *J. Geothermal Research Society of Japan*, 11, pp.203-215.

Moriya, H. and Niitsuma, H., (1994). Precise Location of AE Doublets by Spectral Matrix Analysis of Triaxial Hodogram, *Geophysics*, 59, pp.36-45.

Moriya, H. and Niitsuma, H., (1995). Detection of Micro Shear Wave Splitting in a Dilated Micro Crack Zone by Crosshole Three-Component Seismic Measurement, *Proc. 3rd SEGJ/SEG Int. Symp*, pp.55-62.

Niitsuma, H., (1989). Fracture Mechanics Design and Development of HDR Reservoirs – Concept and Results of the G-project, Tohoku University, Japan, *Int. J. Rock Meck. Min. Sci. and Geomeck. Abstr.*, 26, pp.169-175.

Niitsuma, H. and Saito, H., (1991a). Characterization of a Subsurface Artificial Fracture by the Triaxial Shear Shadow Method, *Geophys. J. Int.*, 107, pp.485-491.

Niitsuma, H. and Saito, H., (1991b). Evaluation of the Three-Dimensional Configuration of a Subsurface Artificial Fracture by the Triaxial Shear Shadow Method, *Geophysics*, 56, pp.2118-2128.

Paillet, F. L. and Cheng, C. H., (1991). Acoustic Waves in Boreholes, *CRC Press, Inc.*

Poupinet, G., Ellsworth, W. and Frechet, J. (1984). Monitoring Velocity Variations in the Crust Using Earthquake Doublets: An Application to Calaveras Fault, California, *J. Geophys. Res.*, 89, pp.7519-5731.

Saito, H. and Hayashi, K., (1999). Detection of a Reservoir Fracture by the Use of Sonic Log Data in EE-4, Higashi-Hachimantai, *Geothermal Resources Council Transaction*, 23, pp.433-437.

Takahashi, H. and Hashida, T. (1992). New Project for Hot Wet Rock Geothermal Reservoir Design Concept. *Proc. 17th Stanford workshop on geothermal reservoir engineering, Stanford*, pp.39-44.

Tanaka, K., Moriya, H., Asanuma, H. and Niitsuma, H., (1999). Detection of Traveltime Delay Caused by Inflation of a Single Artificial Fracture, *Geotherm. Sci. & Tech.*, Vol.6, pp.181-200.

Tang, X. M. and Cheng, C. H., (1989). A Dynamic Model for Fluid Flow in Open Borehole Fractures, *J. Geophys. Res.*, 94, pp.7567-7576.